ELSEVIER

Local production of $O_2^{\cdot-}$ by NAD(P)H oxidase in the sarcoplasmic reticulum of coronary arterial myocytes: cADPR-mediated Ca^{2+} regulation

Fan Zhang, Si Jin, Fan Yi, Min Xia, William L. Dewey, Pin-Lan Li *

Department of Pharmacology & Toxicology, Medical College of Virginia, Virginia Commonwealth University, VA 23298, United States

Abstract

The present study was designed to determine whether the sarcoplasmic reticulum (SR) could locally produce superoxide ($O_2^{\cdot-}$) via NAD(P)H oxidase (NOX) in coronary arterial myocytes (CAMs) and to address whether cADPR-RyR/Ca^{2+} signaling pathway regulates this local $O_2^{\cdot-}$ production from the SR. Using confocal microscopic imaging analysis in intact single CAMs, a cell-permeable indicator CM-H_2DCFDA for dynamic changes in intracellular ROS (in green color) and a highly selective ER-Tracker™ Red dye for tracking of the SR were found co-localized. A quantitative analysis based on the intensity of different spectra demonstrated a local $O_2^{\cdot-}$ production derived from the SR. M_1-receptor agonist, oxotremorine (Oxo) and a Ca^{2+} ionophore, A23187, time-dependently increased this $O_2^{\cdot-}$ production colocalized with the SR. NOX inhibitors, diphenylene iodonium (DPI) and apocynin (Apo), or superoxide dismutase (SOD) and catalase, and Nox4 (a major intracellular NOX subunit) siRNA all substantially blocked this local production of $O_2^{\cdot-}$, demonstrating an involvement of NOX. This SR-derived $O_2^{\cdot-}$ production was also abolished by the inhibitors of cyclic ADP-ribose (cADPR)-mediated Ca^{2+} signaling, such as nicotinamide (Nicot, 6 mM), ryanodine (Rya, 50 μM) or 8-Br-cADPR (30 μM). However, IP_3 antagonist, 2-APB (50 μM) had no effect. In CAMs transfected with siRNA of ADP-ribosyl cyclase or RyR, this SR $O_2^{\cdot-}$ production was attenuated. Electron spin resonance (ESR) spectromic assay in purified SR also demonstrated the production of $O_2^{\cdot-}$ that was dependent on NOX activity and Ca^{2+} concentrations. These results provide direct evidence that $O_2^{\cdot-}$ could be locally produced via NOX on the SR and that this local $O_2^{\cdot-}$ producing system is controlled by cADPR-RyR/Ca^{2+} signaling pathway.

1. Introduction

NAD(P)H oxidase (NOX) has been reported to be one of major sources of reactive oxygen species (ROS) in the vasculature[1–3]. This vascular redox regulatory enzyme is of characteristics of phagocyte NOX, which is composed of two transmembrane-bounded catalytic proteins of gp91phox and p22phox, and three cytosol-associated subunits of p47phox, p67phox and p40phox. In addition to gp91phox named as Nox2, some other homologues of gp91phox such as Nox1, Nox4 and Nox5 were identified in the vascular cells such as endothelial and smooth muscle cells [3,4]. NOX is now well accepted as an important enzyme that produces $O_2^{\cdot-}$ in the vasculature under physiological and pathological conditions to exert redox regulatory action on vascular function or to produce pathogenic responses.

In vascular smooth muscle cells (VSMCs), many studies have demonstrated that $O_2^{\cdot-}$ is accumulated when NOX is activated [1–3]. This intracellular accumulation of $O_2^{\cdot-}$ led to an assumption that a plasma membrane-bound NOX may produce and release $O_2^{\cdot-}$ into cells, which is different from the orientation of phagocyte NOX [1]. However, the topologic analysis has indicated that membrane-associated NOX should not release $O_2^{\cdot-}$ into cytosol [5]. Recent studies on subcellular localization of vascular NOX have also demonstrated that $O_2^{\cdot-}$ within VSMCs may not be derived from plasma membrane NOX (mNOX), but rather from intracellular compartmental NOXs[3,6,7]. We have recently reported that mNOX in VSMCs produced $O_2^{\cdot-}$ in autocrine or paracrine producing manner when the cells were exposed to different agonists [7]. Using purified sarcoplasmic reticulum (SR) from coronary arterial myocytes

* Corresponding author. Department of Pharmacology and Toxicology, Medical College of Virginia, Virginia Commonwealth University, 410 North 12th Street P.O. Box 980613, United States. Tel.:+1 804 828 4793; fax: +1 804 828 2117.

E-mail address: pli@vcu.edu (P.-L. Li).

(CAMs), we also demonstrated that an NOX is present on the SR, and this oxidase locally activates the cyclic ADP – ribose (cADPR) – sensitive ryanodine receptors/Ca^{2+} (RyR/Ca^{2+}) release channels [3]. cADPR is a novel Ca^{2+} mobilizing second messenger, which is capable of inducing Ca^{2+} release from the SR via activation of RyR in CAMs[8–12]. Oxotremorine, a specific M_1 mAChR agonist, has been demonstrated to stimulate ADP-ribosylcyclase activity (CD38) and increase production of cADPR in vascular smooth muscle cells [13,14]. However, so far it is unknown how the SR NOX system associates with cADPR-RyR/Ca^{2+} signaling pathway in these smooth muscle cells.

The present study was designed to address these questions. First, we directly measured the dynamic changes in ROS production in intact CAMs by confocal microscopy using CM-H$_2$DCFDA as a cell-permeable green indicator for ROS and a highly selective ER-Tracker™ red dye for labeling of the SR. A spectrum-based analysis was used to differentiate ROS production derived from the SR or other sources when these cells were stimulated by M1-agonist. Second, we examined the role of NOX in O_2^- production from the SR by using its inhibitors and siRNA of Nox4. To explore the mechanism regulating this SR NOX activity, we tested whether this enzyme is controlled by local Ca^{2+} level and corresponding Ca^{2+} signaling molecules. Using electron spin resonance (ESR) spectrometry, the sensitivity of the SR NOX was analyzed to further determine the Ca^{2+} regulation of NOX activity on the SR.

2. Materials and methods

2.1. Isolation and culture of CAMs

The bovine CAMs were cultured as described previously [14–16]. In brief, bovine intramyocardial coronary arteries from left anterior descending artery were dissected and rinsed with 5% FBS in medium 199 containing 25 mM HEPES with 1% penicillin, 0.3% gentamycin, and 0.3% nystatin. The arterial lumen was filled with 0.4% collagenase in medium 199. After 30 min of incubation at 37 °C, the arteries were flushed with medium199 to denude the endothelium. The strips of denuded arteries were then cut into small pieces and placed into gelatin-coated flasks with medium 199 containing 10% FBS with 1% L-glutamine, 0.1% tyrosin, and 1% penicillin–streptomycin for 3–5 days until CAMs migration to the flasks. Once growth was established, the arteries were removed and cells were continuously grown in medium 199 containing 20% FBS. The identification of CAMs was based on positive staining by an anti-α-actin antibody. All studies were performed with cells of passage of 2–4.

2.2. Confocal fluorescent microscopic detection of ROS localized around the SR in CAMs

Intracellular ROS production around the SR was monitored by their trapping with 5-(and-6)-chloromethyl-2', 7'-dichlorodihydrofluorescein diacetate, acetyl ester (CM-H$_2$DCFDA) and simultaneous labeling of the SR by ER-Tracker™ red dye using confocal laser scanning microscopy [7]. Subconfluent CAMs plated on the Φ35 mm cell culture plates were washed for three times with Hanks' buffered saline solution (HBSS) that contains (in mM): 137 NaCl, 5.4 KCl, 4.2 NaHCO$_3$, 3 Na$_2$HPO$_4$, 0.4 KH$_2$PO$_4$, 1.5 CaCl$_2$, 0.5 MgCl$_2$, 0.8 MgSO$_4$, 10 glucose, 10 HEPES (pH 7.4), then incubated at 37 °C with 5% CO$_2$ in the same HBSS buffer containing 1 μM ER-Tracker™ red dye for 15 min, followed by adding ROS detection agent CM-H$_2$DCFDA to a final concentration of 1 μM and continuing to incubate for another 15 min. To examine the effects of $O_2^{\cdot-}$ scavengers, NAD(P)H oxidase inhibitor, ADP-ribosyl cyclase antagonist, or the SR Ca^{2+} release channel blockers on the Oxotremorine(Oxo)-

induced intracellular ROS production, CAMs loaded with both dyes were pretreated with polyethylene-glycol (PEG)-conjugated O_2^- dismutase (PEG-SOD; 200 U/ml) [17] plus polyethylene-glycol (PEG)-conjugated catalase (CA; 200 U/ml) [18], diphenylene iodonium (DPI; 50 μM), ryanodine (Ryr; 50 μM) or 8-Br-cADPR (30 μM) for 15 min, respectively in different groups of cells and then Oxo-induced ROS production was re-determined. Confocal fluorescent microscopic images were acquired by an Olympus Fluoview System (version 4.2, FV300), which consists of an Olympus BX61WI inverted microscope with an Olympus Lumplan F1×60, 0.9 numerical aperture, and water-immersion objective. Real-time ROS generation was detected as a result of H$_2$DCF oxidation (Green image) by a single z-section, or 0.1-μm sections with excitation and emission wavelengths of 488 and 515 nm, and the staining of SR (Red image) was simultaneously recorded at excitation/emission of 587/615 nm. The subcellular source of ROS was determined by overlaying the ROS green image and SR organelle red image and then the merged images were analyzed off line by using co-localization function of Image Pro-Plus software. For each group of images, the intensity of different color spectrum areas was quantitated. Yellow spots were considered as ROS co-localized around the SR relative to green areas that represent intracellular global ROS or ROS from other resources. The relative fluorescence intensity to basal level before any stimuli was used as normalized fluorescence intensity to present the production of ROS.

2.3. RNA interference of Nox4, ADP-ribosyl cyclase and Ryr/Ca^{2+} receptor in CAMs

In addition to pharmacological intervention, RNA interference was also performed to silence the genes coding NOX subunits dominantly expressed in the SR, Nox4, ADP-ribosyl cyclase and ryanodine receptor 2 (RyR2) in CAMs to further demonstrate that NOX is responsible for the local O_2^- production around the SR and cADPR/RyR Ca^{2+} signaling pathway in the regulation of SR NOX activity. Three pairs of small inhibitory RNA (siRNA) for each gene were chosen using QIAGEN siRNA design program and synthesized and double-stranded by Xeragon. These pairs of siRNA were tested for knocking down specific gene to find a most efficient pair of siRNA for our experimental protocols. A scrambled RNA or Xeragon library scrambled RNA was synthesized for negative control. The most effective pair of siRNA for targeting CD38 (NM_175798) consisted of AAGCGATCAGGCAGGCATTCA and its countpartner; for RyR2 (XM_617538) was AACTGCCAGAGCCAGTAAAAT; and for Nox4 (XM_614713) was AAGACCTGGCCAGTATATATTAT. siRNA transfection was performed according to the manufacturer's instruction in Qiagen TransMessenger kit and as we described previously [7].

2.4. Preparation of purified SR from bovine coronary arterial smooth muscle

Fresh bovine hearts were obtained from a local abattoir, and the coronary arteries were rapidly dissected, and SR-enriched microsomes (SR membrane) of these arteries were prepared as we described previously [3,10,11]. Briefly, the dissected coronary arteries (outer diameter 500–1000 μm) were cleared of surrounding fat and connective tissues. The arteries were cut open along the longitudinal axis and pinned lumen side up to a Sylgard-coated dish containing ice-cold HEPES buffered physiological saline solution (in mM: 140 NaCl, 4.7 KCl, 1.6 CaCl$_2$, 1.17 MgSO4, 1.18 NaH$_2$PO4, 5.5 glucose, and 10 HEPES, pH 7.4). A sharp blade was used to scratch endothelial cells from the arteries. Then the segments of the arteries were cut into small (2- to 3-mm-long) pieces and homogenized with a Polytron (Brinkman) in ice-cold MOPS buffer (0.9% NaCl, 10 mM MOPS (pH 7.0), 2 M leupeptin, and 0.8 M benzamidine). The homogenate was centrifuged at 4000 g for 20 min at 4 °C, and the supernatant was further centrifuged at 8000 g for 20 min at 4 °C and then at 40,000 g for 30 min. The pellet, termed the crude SR membrane, was resuspended in the SR solution (0.9% NaCl, 0.3 M sucrose, and 0.1 M phenylmethylsulfonyl fluoride) [10]. The crude SR was further fractionated on a discontinuous sucrose gradient [3,19,20]. The following sucrose solutions (percent by weight) containing 10 mM HEPES, pH 7.0, were layered sequentially in a centrifuge tube (model SW28, Beckman) as follows: 4 ml of 45%, 7 ml of 40%, 12 ml of 35%, 7 ml of 30%, and 4 ml of 27%. Crude SR (30 mg) was layered on top of the gradient, and the tube was spun at 64,000 g overnight. A fraction from 37–40% sucrose contained the purified SR, which was collected and diluted in

MOPS buffer [0.9% NaCl, 10 mM MOPS (pH 7.0), 2 μM leupeptin, and 0.8 μM benzamidine] and subjected to further centrifugation at 40,000 g for 90 min at 4 °C. The pellet was resuspended in the SR solution, aliquoted, frozen in liquid N2, and stored at 80 °C.

2.5. ESR Detection of O_2^-

Purified SR from bovine coronary artery was suspended in modified Kreb's_HEPEs buffer containing deferoxime (100 μM) [7,21]. The NOX activity to produce O_2^- in the SR was examined by addition of 1 mM NADH as a substrate in the 100 μg purified SR mixture and incubated for 15 min, and then supplied with 1 mM O_2^- — specific spin trap 1-hydroxy-3-methoxycarbonyl-2,2,5,5-tetramethylpyrrolidine(CMH) in the presence or absence of NOX inhibitors apocynin (Apo, 100 μM) or SOD (200 U/ml) or its mimetic Tiron (1 mM). The SR mixture loaded in glass capillaries was immediately analyzed for O_2^- production kinetically for 10 min. The ESR settings were as follows: biofield, 3350; field sweep, 60 G; microwave frequency, 9.78 GHz; microwave power, 20 mW; modulation amplitude, 3 G; 4,096 points of resolution; receiver gain, 500; and kinetic time, 10 min.

2.6. Statistics

Data are expressed as means±SE. The significance of the differences in mean values between and within multiple groups such as multiple time points was examined by ANOVA for repeated measures followed by Duncan's multiple range test. Student's t-test was used to evaluate the statistical significance of differences between two paired observations. $P<0.05$ was considered statistically significant.

3. Results

3.1. Localized ROS production by the SR in response to Oxo

Using confocal microscopic analysis, we dynamically monitored the cytosolic H_2O_2 level by measuring oxidized-H2DCFDA green fluorescence and at the same time we also recorded SR staining by ER-Tracker red dye. Fig. 1A shows typical sequential fluorescent images when a CAM received Oxo at 80 μM. It was found that green fluorescence intensity of H2DCFDA markedly increased in a time-dependent manner, but the red fluorescence staining of the SR remains unchanged. The merged images showed a number of yellow spots, which also increased in a time-dependent manner. These spots represent colocalization of O_2^- with the SR, and increased intensity indicated ROS derived from the SR. In addition to yellow areas in the merged images, rest areas of green fluorescence represent non-SR-derived ROS or global ROS levels. To quantitate SR-derived ROS and global or non-SR ROS, we used the Image-Pro Plus version 6.0 software to analyze the yellow spot intensity as well as green staining intensity from the merged image based on the color spectra. Fig. 1B summarized the results. The normalized yellow fluorescence intensity significantly increased by more than 4 folds when CAMs were exposed to Oxo over the 12 min. The global ROS levels as shown by green staining also increased with a less intensity than local ROS around the SR.

3.2. Effects of NOX inhibitors and Nox4 siRNA on SR-derived ROS production

To demonstrate that ROS derived from the SR are due to O_2^- production by activation of SR NOX, we tested the effects of SOD
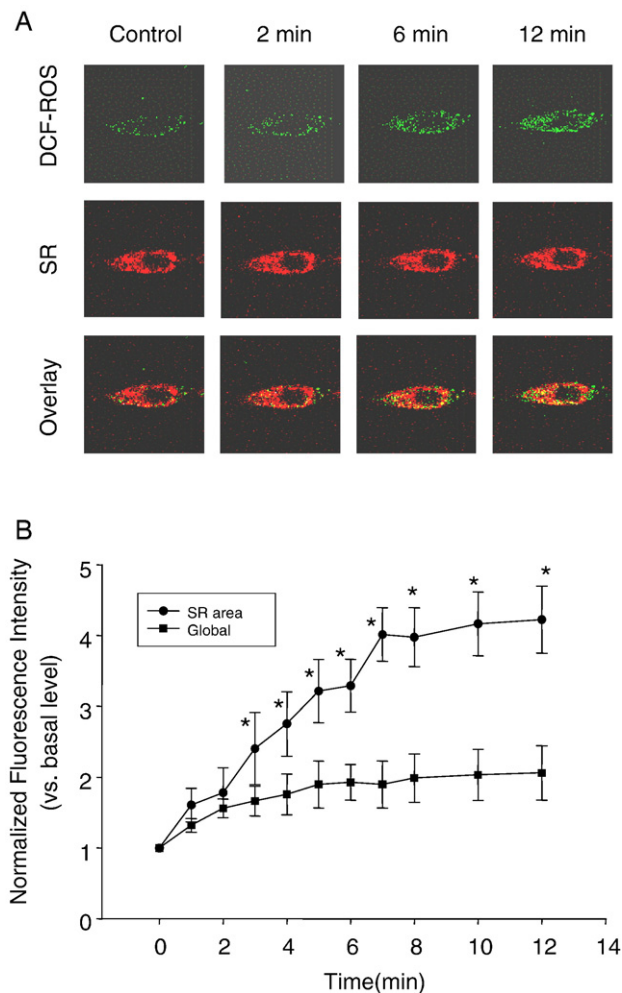

Fig. 1. Time-dependent local superoxide (O_2^-) production from sarcoplasmic reticulum (SR) in intact coronary arterial myocytes (CAMs) by confocal fluorescence microscopy under the treatment of 80 μM oxotremorine (Oxo). CAMs were loaded with ER-Tracker™ dyes for the trace of SR (red) and CM-H2DCFDA (DCF) for H_2O_2 detection as ROS indicator (green). A: Typical cell images with green fluorescence for ROS detection and red fluorescence for SR staining. The merged images with yellow spots or staining show colocalization of ROS derived from the SR (Colour images available online). B: Summarized digitized data dissecting SR-derived ROS level (yellow in images) from global ROS or non-SR ROS (green in images). $n=6$, *$P<0.05$ compared with basal level.

combined with catalase and NOX inhibition or downregulation on local ROS levels. First, cell permeable polyethylene-glycol (PEG)-conjugated O_2^- dismutase (PEG-SOD) [17] and poly-ethylene-glycol (PEG)-conjugated catalase (PEG-Catalase) [18] were used in combination when CAMs were stimulated by Oxo. It was found that SOD and Catalase significantly blocked ROS increase colocalized with the SR (Fig. 2B).

Then, we tested whether NOX is involved in local ROS production using its inhibitors, DPI and Nox4 siRNA. The successful inhibitory effects of Nox4 siRNA on the expression of this Nox isoform was confirmed by the Western blot analysis in CAMs (anti-Nox4 antibody, Santa Cruz); It was shown that the expression of Nox4 was almost completely disrupted by its siRNA, as shown in Fig. 2A. The results from these experiments were also summarized in Fig. 2B, showing that NOX inhibition
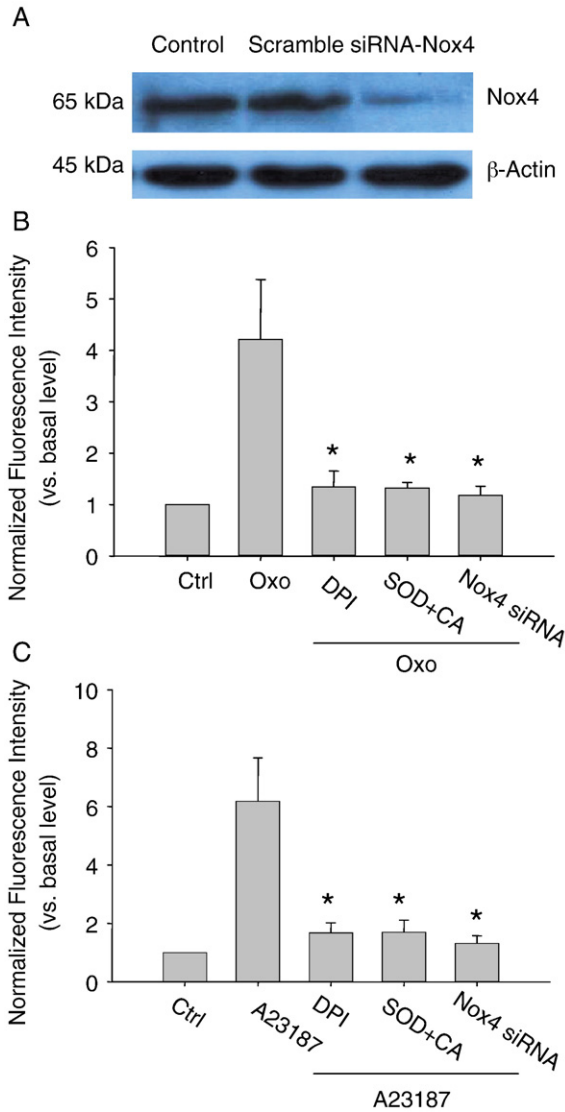
A

Fig. 2. Effects of ROS scavengers, NAD(P)H oxidase inhibitor or Nox4 siRNA on SR-derived O_2^- production in CAMs by confocal fluorescence microscopy assay. A: Western blot analysis shows knockdown of Nox4 by its siRNA in CAMs. B: Summarized data showing the effects of PEG-SOD, NAD(P)H oxidase inhibitor, DPI and Nox4 siRNA on SR-derived O_2^- production induced by Oxo (80 μM). C: Summarized data showing the effects of PEG-SOD, NAD(P)H oxidase inhibitor, DPI and Nox4 siRNA on SR-derived O_2^- production induced by A23187 (1 μM). $n=6$, *$P<0.05$ compared with Oxo or A23187 alone group.

or gene silencing almost completely abolished the SR-derived ROS production.

In addition to the use of Oxo as agonist, we also tested the effects of the NOX inhibition or gene silencing on ROS production induced by another stimulator of NOX in CAMs, namely, Ca^{2+} ionophere, A23187 [22]. It was found that A23187 (1 μM) markedly increased local ROS production in CAMs. When these cells were pretreated with PEG-SOD and PEG-catalase in combination, this A23187-induced local ROS production was substantially attenuated. Similarly, inhibition of NOX activity by DPI or silencing its expression by Nox4 siRNA also significantly blocked this local ROS production induced by A23187 (Fig. 2C).
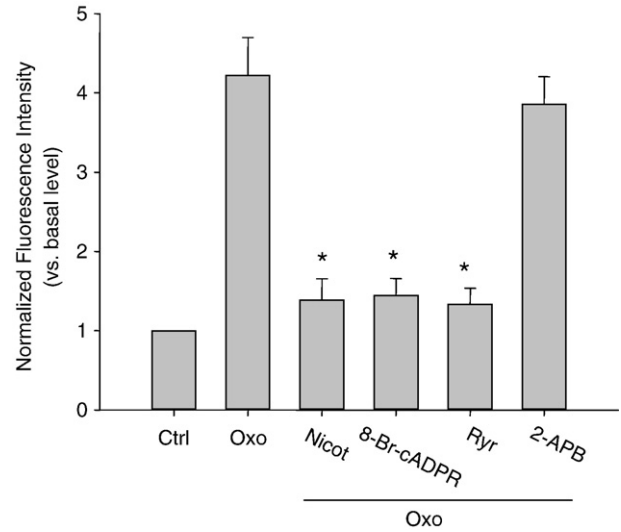

Fig. 3. Effects of cADPR-RyR/Ca^{2+} signaling pathway inhibition on SR-derived O_2^- production in CAMs by confocal fluorescence microscopy assay. ADP-ribosyl cyclase inhibitor, nicotinamide (Nicot.; 6 mM), cADPR antagonist, 8-Br-cADPR (30 μM), or RyR/Ca^{2+} release channel inhibitor, ryanodine (Ryr; 50 μM) was used. 2-aminoethoxydiphenyl borate (2-APB; 50 μM) was also used as an antagonist of Ins(1,4,5)P_3 receptor. $n=6$, *$P<0.05$ compared with Oxo alone group.

3.3. Effect of cADPR-RyR-Ca^{2+} signaling pathway inhibitors on local O_2^- production from the SR

Given the Ca^{2+} sensitivity of NOX activity, we determined whether cADPR-RyR-Ca^{2+} signaling pathway contributes to the activation of local ROS production via NOX on the SR. It was found that ADP-ribosyl cyclase inhibition by nicotinamide (Nicot.), cADPR antagonist, 8-Br-cADPR, or RyR-Ca^{2+} release channel blockade by ryanodine at a large dose (Rya), Oxo-induced O_2^- production significantly decreased by 3.03, 2.92 and 3.17 folds, respectively, compared to Oxo alone. These results were summarized in Fig. 3. It was also found that 2-aminoethoxydiphenyl borate (2-APB; 50 μM), the inhibitor of
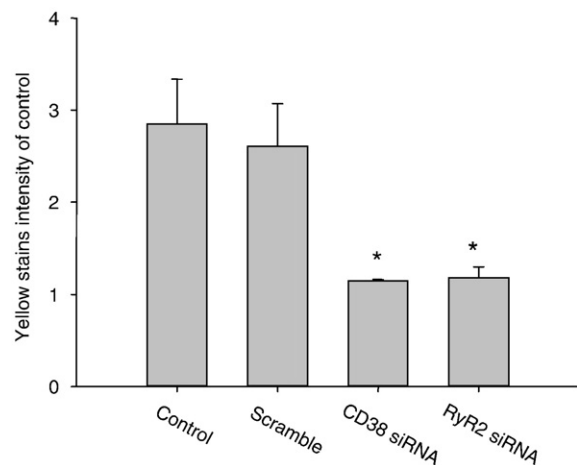

Fig. 4. Effects of RNA interference of ADP-ribosyl cyclase(CD38) or/and RyR2 gene on SR-derived O_2^- production in CAMs by confocal fluorescence microscopy. ADP-ribosyl cyclase or RyR2 siRNAs were introduced before experiments using siLentFect™ lipid followed by 80 μM Oxo treatment. $n=6$, *$P<0.05$ compared with control.

Ins(1,4,5)P$_3$ receptor, had no effects on the Oxo-induced O$_2^-$ production from the SR.

3.4. Effects of cADPR-RyR/Ca^{2+} pathway RNA interference on SR-derived O$_2^-$ production

To further address the regulatory role of cADPR-RyR/Ca^{2+} signaling pathway in SR production of O$_2^-$, we examined the effects of RNA interference of two genes coding ADP-ribosyl cyclase and RyR-2. In these experiments, CAMs were pretreated with siRNA of ADP-ribosyl cyclase or RyR receptor and satisfied interference efficiency of siRNA had been confirmed by real time RT-PCR of their corresponding mRNA and Western blot analysis of their proteins (data not shown). Under confocal fluorescence microscope, the intensity of yellow stains produced by green H$_2$O$_2$ dye was significantly reduced in either ADP-ribosyl cyclase or RyR receptor siRNA-treated CAMs. Normalized fluorescence intensity of this colocalization before and after siRNA treatment was presented in Fig. 4.

3.5. Ca^{2+} regulation of NAD(P)H oxidase-derived O$_2^-$ production from purified SR analyzed by ESR

Using ESR spectrometric assay, we demonstrated that NAD(P)H oxidase was functioning in the purified SR from bovine
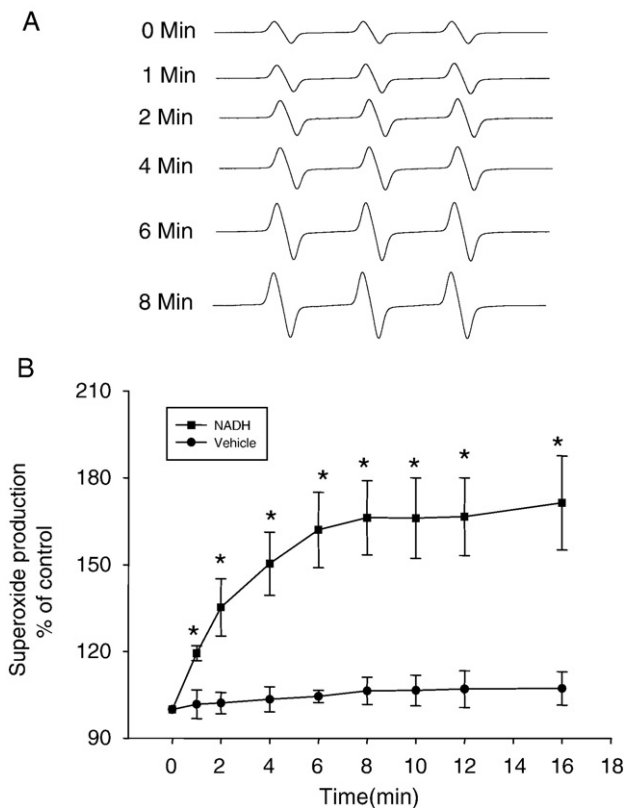

Fig. 6. Effects of O$_2^-$ scavengers, NAD(P)H oxidase inhibitors or Ca^{2+} dependence on O$_2^-$ production in the purified SR from bovine CAMs by ESR assay. $n=6$, *, #$P<0.05$ compared with NADH alone group.

CAMs. NAD(P)H-dependent O$_2^-$ production was measured using NADH as substrate. NADH was chosen as the substrate because of the preference of SR Nox4-containing NAD(P)H oxidase for NADH [23,24], rather than NADPH. Fig. 5A shows representative ESR spectrographs of O$_2^-$ trapped by 1-hydroxy-3-methoxycarbonyl-2,2,5,5-tetramethylpyrrolidine (CMH) in the reaction mixture with 1 mM NADH. As summarized in Fig. 5B, O$_2^-$ production in these purified SR was significantly increased by 1.7 folds over a 16-min reaction compared to control. A rapid increase in O$_2^-$ production was observed at the first 5 min of the reaction. This SR-derived O$_2^{\cdot-}$ production was almost blocked by NAD(P)H oxidase inhibitors Apo (100 µM), SOD (200 U/ml), and its mimetic Tiron (1 mM) (Fig. 6). To determine the Ca^{2+} sensitivity of this SR enzyme, we examined the effects of different Ca^{2+} concentrations on SR O$_2^-$ production. The results are presented in Fig. 6. In the presence of 1 mM NADH, Ca^{2+} increases in the reaction mixtures produced a concentration-dependent enhancement of O$_2^-$ production as measured by ESR trapping. A 1.5 fold increase was reached at 1 µM of Ca^{2+} in the reaction.

4. Discussion

There is increasing evidence that NAD(P)H oxidase is a major source of O$_2^-$ in the vasculature and that O$_2^-$ from this enzyme serves as an important physiological redox signaling molecule to participate in the regulation of vascular function [1,25–28]. In vascular smooth muscle cells (VSMCs), recent studies have reported that there are membrane-bound and intracellular non-mitochondrial NAD(P)H oxidases, which are all capable of producing O$_2^-$ and contributing to intracellular O$_2^-$ concentrations in these cells [1,29]. However, it remains unknown how the intracellular O$_2^-$ concentrations are determined by this NAD(P)H oxidase in VSMCs. Although a

Fig. 5. Time-dependent O$_2^-$ production of purified SR from bovine CAMs detected by electron spin resonance (ESR) spectrometry. A: representative ESR spectrograph of O$_2^-$ trapped by 1-hydroxy-3-methoxycarbonyl-2,2,5,5-tetramethylpyrrolidine (CMH) in the reaction mixture with NADH as substrate. B: Summarized data showing time-dependent increase in O$_2^-$ production from the purified SR. $n=6$, *$P<0.05$ compared with control.
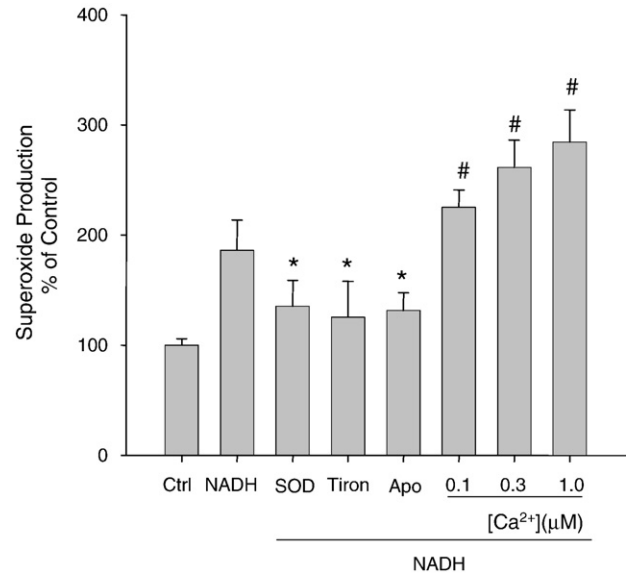
membrane-bound NAD(P)H oxidase is assumed to produce O_2^- toward the inside of these cells [1], the topology of NAD(P)H oxidase subunits indicates that membrane-associated NAD(P)H oxidase should not release O_2^- into cytosol. More recent studies on subcellular localization of vascular NAD(P)H oxidase subunits also demonstrated that O_2^- within VSMCs may not be derived from plasma membrane NAD(P)H oxidase [5,24], but rather from intracellular compartmental NAD(P)H oxidase [3,6]. Although there are reports about the localization of NAD(P)H oxidases in different cellular organelles such as mitochondria, SR and Golgi apparatus, little is known how O_2^- production in these intracellular compartments are activated or regulated in VSMCs.

In the present study, we characterized an NAD(P)H oxidase-dependent O_2^- production from the SR in intact CAMs and explored the regulatory mechanisms associated with a novel Ca^{2+} signaling pathway, namely, the role of cADPR-mediated Ca^{2+} mobilization mechanism. In these experiments, we used M_1 agonist, oxotremorine (Oxo), to stimulate O_2^- production via NAD(P)H oxidase in CAMs. The reason for the use of this M_1 agonist, Oxo, is due to its strong action inducing O_2^- production and vasoconstriction in denuded bovine coronary arteries [7,30]. In particular, previous studies have shown that bovine coronary arteries are insensitive to classical vasoconstrictors such as angiotensin II, norepinephrine, and vasopressin [7,31–33] and therefore the vasoconstrictor action of this M_1 agonist is unique in studying the mechanism of bovine coronary vasoconstriction. This compound-induced vasoconstriction was often found to be accompanied by O_2^- production, and the latter may further enhance or amplify the vasoconstriction in these arteries [3,30,34]. In addition, many studies have demonstrated that M_1 receptor activation produces vasoconstriction primarily through cADPR-RyR Ca^{2+} signaling pathway in coronary arteries [13,35]. Based on these findings, it is proposed that M_1 agonist is a unique tool compound for studies of Ca^{2+} and redox signaling and their interactions in CAMs [30,36].

Using Confocal microscopy, we first detected O_2^- production in the SR of intact CAMs. In these experiments, CAMs were treated by Oxo, and O_2^- production in the SR were measured by co-staining of CM-H$_2$DCFDA (green) for H_2O_2 and ER-Tracker (red) for the SR. CM-H$_2$DCFDA was used as a general indicator of intracellular ROS formation, primarily derived from O_2^- production. Although dihydroethidium (DHE) was widely used to directly measure intracellular O_2^- production, which is based on that DHE is converted to ethidium bromide(EB) upon oxidation by superoxide, and these oxidized EB translocated to the nucleous where it intercalates with DNA to generate red fluorescence. It is obvious that the site of accumulation of bright-red fluorescence from oxidized DHE and DNA complex is not a suitable indicator of the location where ROS were produced [37]. In contrast, CM-H$_2$DCFDA is able to localize cellular production of ROS within the tissue, and the sensitivity to detect ROS within a single cell, these strengths has made CM-H$_2$DCFDA widely used in the measurement of intracellular localized ROS by imaging assay [38,39]. With the help of an Image-Pro Plus analysis software (version 6.0), the intensity of spots with different colors or

spectra could be quantified in overlaid fluorescent confocal images. By measuring the intensity of yellow spots formed by overlay of CM-H$_2$DCFDA green fluorescence and SR-tracker red fluorescence, the level of H_2O_2 primarily derived from the SR could be detected. By analysis of green fluorescence intensity, total H_2O_2 or H_2O_2 from other cellular resources was assessed. It was found that Oxo time-dependently increased H_2O_2 production around the SR, as measured by yellow fluorescent intensity. Although this M_1-agonist also increased global ROS production, as measured by green fluorescence intensity, the increase in SR-derived ROS was more significantly intensive. In the presence of cell permeable of PEG-SOD and PEG-catalase, Oxo-induced SR production of ROS was substantially blocked. These results suggest that this confocal microscopic local assay does detect O_2^- production from the SR of intact CAMs. Although O_2^- or other ROS production was reported in different cellular compartments [3,40], many of previous studies used isolated organelles such as mitochondria and SR to analyze related ROS or enzyme activity [3,40]. The confocal microscopic analysis of local production of ROS has been reported only in studies of mitochondrial redox status or ROS release from this organelles in intact cells [39,41,42]. In those studies, CM-H$_2$DCFDA was also used to localize ROS derived from the mitochondria with the help of quantitative analysis of its localization with mitochondrial markers. To our knowledge, the present study represents the first report to use such technique to detect ROS derived from the SR of intact CAMs.

It is well known that several potential enzymatic sources of O_2^- in the cardiovascular system, such as xanthine oxidase, mitochondrial respiratory chain, arachidonic acid metabolizing system, uncoupled NO synthase, and NAD(P)H oxidase [43,44] may contribute to the production of O_2^- or ROS within different cells. However, accumulating evidence has indicated that non-mitochondrial NAD(P)H oxidase may be a major resource for intracellular ROS in vascular smooth muscle cells and thereby this enzyme system play an important role in the regulation of vascular smooth muscle function under physiological and pathological conditions [1,25–28]. In this regard, previous studies have reported that Nox4 is a major catalytic subunit of NAD(P)H oxidase in different organelle of vascular smooth muscle cells including the SR [3,7,24]. In the present study, we tested whether this NAD(P)H oxidase contributes to the ROS production from the SR. We performed confocal analysis of SR-derived ROS production in CAMs in the absence or presence of a specific inhibitor DPI of this enzyme or Nox4 siRNA. It was demonstrated that ROS production from the SR was markedly reduced when NAD(P)H oxidase was inhibited or a Nox4 siRNA was introduced, no matter whether Oxo or A23187 was used as stimuli. These results suggest that NAD(P)H oxidase is primarily responsible for the production of ROS from the SR. In previous studies using isolated SR, the expression and activity of an NAD(P)H oxidase were also detected in cardiomycytes and smooth muscle cells [3,45]. Our present results further support the view that this NAD(P)H oxidase is functioning even when vascular smooth muscle produces vasomotor response to physiological stimuli.

Another important question being addressed in the present study is whether the activity of NAD(P)H oxidase on the SR is regulated by its Ca^{2+} signaling mechanisms. Since NAD(P)H oxidase has been reported to be a Ca^{2+}-dependent enzyme for O_2^- production, it is possible that a local Ca^{2+} regulatory mechanism may control its activity. To test this hypothesis, we performed a series experiments to examine the possible pathway that may be involved in the regulation of NAD(P)H oxidase activity. First, we tested whether IP_3 or ryanodine-sensitive Ca^{2+} mobilizing pathway has impact on the NAD(P)H oxidase activity. It was found that RyR inhibition rather than IP_3 antagonist blocked Oxo-induced activation of SR NAD(P)H oxidase. Further experiments using RyR2 siRNA also demonstrated that Oxo-induced NAD(P)H oxidase activity was abolished. It seems that NAD(P)H oxidase activity is dependent on RyR activation by Oxo, rather than IP_3R activation. Indeed, previous studies confirmed that Oxo-induced vasoconstrictor response primarily through RyR-mediated Ca^{2+} mobilization from the SR [13,14]. Second, we tested the role of an IP_3-independent Ca^{2+} releasing mechanism, cADPR pathway, in the regulation of SR NAD(P)H oxidase. This cADPR-mediated Ca^{2+} has been also proposed as a major Ca^{2+} mobilizing or vasomotor response during M_1 receptor activation [13,14]. Interestingly, we found that all manipulations of this signaling pathway could block Oxo-induced ROS production from the SR, no matter whether cADPR-producing enzyme was inhibited or its gene silenced, or cADPR antagonist was used. Given that cADPR produces Ca^{2+} mobilization from the SR mainly through RyR activation, these results suggest that NAD(P)H oxidase activity on the SR is associated with cADPR-mediated activation of RyR. It may be proposed that M_1 receptor stimulation by Oxo leads to cADPR production and the latter induces Ca^{2+} releasing and thereby results in local activation of NAD(P)H oxidase on the SR.

Finally, we directly tested the Ca^{2+} sensitivity of NAD(P)H oxidase on the SR isolated from CAMs. Using ESR spectrometry, O_2^- production was analyzed by incubation of the SR with NAD(P)H oxidase substrate, NADH. After validation of this ESR detection for O_2^- production by NAD(P)H oxidase using O_2^- scavengers or different NAD(P)H oxidase inhibitors, we tested whether the SR NAD(P)H oxidase activity is altered by increasing Ca^{2+} concentrations in the reaction mixtures. Consistent with the results reported in other membrane fractions [3,22,46], increases in Ca^{2+} significantly enhanced the activity of NAD(P)H oxidase from the SR. It is obvious that these results provide direct evidence that elevated intracellular Ca^{2+} can be an critical activator of NAD(P)H oxidase, which regulates local generation of O_2^- from the SR. Given the sensitivity of RyR to ROS, this Ca^{2+} activation of NAD(P)H oxidase may constitute an amplification system between Ca^{2+} and redox signaling in CAMs. In this way, Ca^{2+} enhances NAD(P)H oxidase activity to produce O_2^-, and ROS sensitizes RyRs to release more Ca^{2+}, forming a local feedforward regulatory circuit.

In summary, the present study demonstrated that 1) O_2^- was locally derived from SR in response to M_1 agonist in CAMs; 2) SR-derived O_2^- production was blocked by NAD(P)H oxidase inhibitor and Nox4 siRNA; 3) SR-derived O_2^- production was abolished by the inhibitors of ADP-ribosyl cyclase, RyR, and
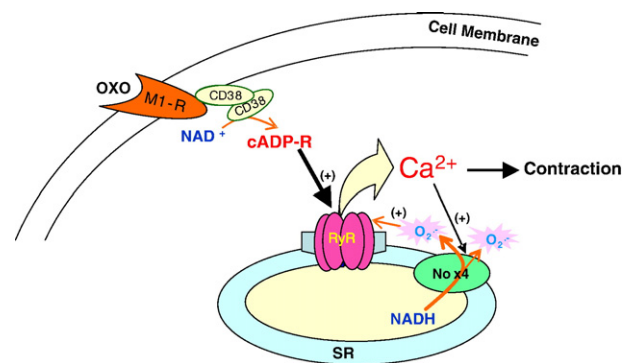

Fig. 7. A schematic diagram showing our conclusion that O_2^- is locally produced from Nox4 in the SR of CAMs in response to M_1 receptor activation and that this local O_2^- production is regulated by cADPR-RyR-Ca^{2+} signaling pathway. Given the great sensitivity of RyRs to redox changes, increased local O_2^- level may enhance the activation of these receptors, leading to a feed forward regulation of both redox and Ca^{2+} signaling in CAMs (Colour diagram available online).

cADPR antagonist but not by IP_3 antagonist; 4) both ADP-ribosyl cyclase and RyR siRNA inhibited O_2^- production from SR; and 5) Purified SR produced O_2^- was dependent on NAD(P)H oxidase in a Ca^{2+} sensitive manner. As shown in a schematic diagram in Fig. 7, we conclude that NAD(P)H oxidase on the SR of intact CAMs is functioning in response to physiological stimuli such as M_1 receptor activation and that this local enzyme is sensitive to intracellular Ca^{2+} regulation associated with cADPR-RyR signaling pathway. Given previous evidence of high sensitivity of RyRs to redox changes, increased O_2^- production may enhance the activity of these receptors releasing more Ca^{2+}. The latter again activates NAD(P)H oxidase on the SR constituting a feed forward mechanism. This interaction of Ca^{2+} and redox signaling around the SR may importantly contribute to Ca^{2+} regulation of coronary arterial smooth muscle and thereby enhance vasoconstrictor responses.

Acknowledgement

References

[1] K.K. Griendling, D. Sorescu, M. Ushio-Fukai, Circ. Res. 86 (5) (2000) 494–501.
[2] K.M. Mohazzab, P.M. Kaminski, M.S. Wolin, Am. J. Physiol. 266 (6 Pt 2) (1994) H2568–H2572.
[3] X.Y. Yi, V.X. Li, F. Zhang, F. Yi, D.R. Matson, M.T. Jiang, P.L. Li, Am. J. Physiol. Heart Circ. Physiol. 290 (3) (2006) H1136–H1144.
[4] C. Patterson, J. Ruef, N.R. Madamanchi, P. Barry-Lane, Z. Hu, C. Horaist, C.A. Ballinger, A.R. Brasier, C. Bode, M.S. Runge, J. Biol. Chem. 274 (28) (1999) 19814–19822.
[5] R.P. Brandes, J. Kreuzer, Cardiovasc. Res. 65 (1) (2005) 16–27.
[6] M.S. Wolin, M. Ahmad, S.A. Gupte, Am. J. Physiol., Lung Cell, Mol. Physiol. 289 (2) (2005) L159–L173.
[7] G. Zhang, F. Zhang, R. Muh, F. Yi, K. Chalupsky, H. Cai, P.L. Li, Am. J. Physiol. Heart Circ. Physiol. 292 (1) (2007) H483–H495.
[8] H.C. Lee, R. Aarhus, R. Graeff, M.E. Gurnack, T.F. Walseth, Nature 370 (6487) (1994) 307–309.
[9] H.C. Lee, R. Aarhus, R.M. Graeff, J. Biol. Chem. 270 (16) (1995) 9060–9066.

[10] P.L. Li, W.X. Tang, H.H. Valdivia, A.P. Zou, W.B. Campbell, Am. J. Physiol. Heart Circ. Physiol. 280 (1) (2001) H208–H215.

[11] W.X. Tang, Y.F. Chen, A.P. Zou, W.B. Campbell, P.L. Li, Am. J. Physiol. Heart Circ. Physiol. 282 (4) (2002) H1304–H1310.

[12] J. Geiger, A.P. Zou, W.B. Campbell, P.L. Li, Hypertension 35 (1 Pt 2) (2000) 397–402.

[13] Z.D. Ge, D.X. Zhang, Y.F. Chen, F.X. Yi, A.P. Zou, W.B. Campbell, P.L. Li, J. Vasc. Res. 40 (1) (2003) 28–36.

[14] F. Zhang, G. Zhang, A.Y. Zhang, M.J. Koeberl, E. Wallander, P.L. Li, Am. J. Physiol. Heart Circ. Physiol. 291 (1) (2006) H274–H282.

[15] P.L. Li, C.L. Chen, R. Bortell, W.B. Campbell, Circ. Res. 85 (4) (1999) 349–356.

[16] P.L. Li, A.P. Zou, W.B. Campbell, Am. J. Physiol. 275 (3 Pt 2) (1998) H1002–H1010.

[17] U. Landmesser, H. Cai, S. Dikalov, L. McCann, J. Hwang, H. Jo, S.M. Holland, D.G. Harrison, Hypertension 40 (4) (2002) 511–515.

[18] E.N. Defoort, P.M. Kim, L.M. Winn, Mol. Pharmacol. 69 (4) (2006) 1304–1310.

[19] G. Salama, J. Abramson, J. Biol. Chem. 259 (21) (1984) 13363–13369.

[20] R. Xia, J.A. Webb, L.L. Gnall, K. Cutler, J.J. Abramson, Am. J. Physiol. Cell. Physiol. 285 (1) (2003) C215–C221.

[21] K. Chalupsky, H. Cai, Proc. Natl. Acad. Sci. U. S. A. 102 (25) (2005) 9056–9061.

[22] R.J. Smith, S.S. Iden, Inflammation 5 (3) (1981) 177–192.

[23] T. Kobayashi, V.S. Zinchuk, T. Okada, H. Wakiguchi, T. Kurashige, H. Takatsuji, H. Seguchi, Histochem. Cell Biol. 113 (4) (2000) 251–257.

[24] B. Lassegue, R.E. Clempus, Am. J. Physiol. Regul. Integr. Comp. Physiol. 285 (2) (2003) R277–R297.

[25] K.M. Mohazzab, M.S. Wolin, Am. J. Physiol. 267 (6 Pt 1) (1994) L815–L822.

[26] S. Rajagopalan, S. Kurz, T. Munzel, M. Tarpey, B.A. Freeman, K.K. Griendling, D.G. Harrison, J. Clin. Invest. 97 (8) (1996) 1916–1923.

[27] Y.J. Suzuki, G.D. Ford, J. Mol. Cell. Cardiol. 31 (2) (1999) 345–353.

[28] J.J. Zulueta, F.S. Yu, I.A. Hertig, V.J. Thannickal, P.M. Hassoun, Am. J. Respir. Cell Mol. Biol. 12 (1) (1995) 41–49.

[29] H. Cai, Circ. Res. 96 (8) (2005) 818–822.

[30] A.Y. Zhang, F. Yi, E.G. Teggatz, A.P. Zou, P.L. Li, Microvasc. Res. 67 (2) (2004) 159–167.

[31] A.Y. Zhang, F. Yi, G. Zhang, E. Gulbins, P.L. Li, Hypertension 47 (1) (2006) 74–80.

[32] D.X. Zhang, F.X. Yi, A.P. Zou, P.L. Li, Am. J. Physiol. Heart Circ. Physiol. 283 (5) (2002) H1785–H1794.

[33] P.L. Li, M.W. Jin, W.B. Campbell, Hypertension 31 (1 Pt 2) (1998) 303–308.

[34] H.L. Wilson, M. Dipp, J.M. Thomas, C. Lad, A. Galione, A.M. Evans, J. Biol. Chem. 276 (14) (2001) 11180–11188.

[35] H. Higashida, S. Yokoyama, M. Hashii, M. Taketo, M. Higashida, T. Takayasu, T. Ohshima, S. Takasawa, M. Okamoto, M. Noda, J. Biol. Chem. 272 (50) (1997) 31272–31277.

[36] A.Y. Zhang, P.L. Li, J. Cell. Mol. Med. 10 (2) (2006) 407–422.

[37] T. Yeung, N. Touret, S. Grinstein, Curr. Opin. Microbiol. 8 (3) (2005) 350–358.

[38] S. Dikalov, K.K. Griendling, D.G. Harrison, Hypertension 49 (4) (2007) 717–727.

[39] J.W. Zmijewski, D.R. Moellering, C. Le Goffe, A. Landar, A. Ramachandran, V.M. Darley-Usmar, Am. J. Physiol Heart Circ. Physiol. 289 (2) (2005) H852–H861.

[40] Y. Liu, H. Zhao, H. Li, B. Kalyanaraman, A.C. Nicolosi, D.D. Gutterman, Circ. Res. 93 (6) (2003) 573–580.

[41] S. Lecour, E. Van der Merwe, L.H. Opie, M.N. Sack, J. Cardiovasc. Pharmacol. 47 (1) (2006) 158–163.

[42] M.J. Jou, T.I. Peng, H.Y. Wu, Y.H. Wei, Ann. N. Y. Acad. Sci. 1042 (2005) 221–228.

[43] M.S. Wolin, Microcirculation 3 (1) (1996) 1–17.

[44] M.S. Wolin, M. Ahmad, S.A. Gupte, Kidney Int. 67 (5) (2005) 1659–1661.

[45] C. Hidalgo, P. Aracena, G. Sanchez, P. Donoso, Biol. Res. 35 (2) (2002) 183–193.

[46] S.G. Carriedo, H.Z. Yin, S.L. Sensi, J.H. Weiss, J. Neurosci. 18 (19) (1998) 7727–7738.